Archives of Environmental Protection
Vol. 51 no. 1 pp. 32–44

PL ISSN 2083-4772
DOI:10.24425/aep.2025.153747

Improving geopolymers with multi-walled carbon nanotubes for simultaneous adsorption of lead and anthracene from rainwater

Anna Marszałek[1], Noura Fathy Abdel Salam[2], Gabriela Kamińska[1]*

[1]Silesian University of Technology, Gliwice, Poland
[2]Cairo University, Egypt

* Corresponding author's e-mail: gabriela.kaminska@polsl.pl

Keywords: rainwater, lead, anthracene, geopolymer, carbon nanotubes, and adsorption

Abstract: The aim of this study was to prepare and assess the effectiveness of a geopolymer doped with multi-walled carbon nanotubes functionalized with carboxyl groups (GEO+MWCNT) for removing lead (Pb(II)) and anthracene (ANT) from rainwater. Characterization of the GEO+MWCNT demonstrated an increased specific surface area and microporosity compared to the pristine geopolymer (GEO). Adsorption experiments revealed that GEO+MWCNT achieved higher removal efficiencies for Pb(II) and ANT compared to GEO alone. The maximum removal rates of lead and anthracene by GEO+MWCNT were 100% and 87.5%, respectively, compared to 71.5% and 76.2% for GEO. For GEO+MWCNT, lead removal was 78.2% in anthracene-containing solutions and 86.7% in anthracene-free rainwater. The optimal removal of Pb(II) occurred at pH 8. The adsorption kinetics followed a pseudo-second-order model, indicating a complex mechanism involving physical adsorption, chemisorption, and electrostatic attraction. These findings suggest that geopolymers, particularly when combined with MWCNT-COOH, have significant application potential for rainwater purification processes.

Introduction

In recent years, there has been growing interest in using rainwater as an alternative water source (Khanal et al. 2020, Murat-Błażejewska and Błażejewski 2020). A key challenge in this field is ensuring the quality of water collected from roofs, which can be contaminated with heavy metals and polycyclic aromatic hydrocarbons (PAHs) (Mojir et al. 2019). Heavy metals such as lead, cadmium, and mercury are toxic pollutants that can negatively affect the environment and human health (Tan et al. 2019, Li et al. 2022). Their presence in rainwater is primarily attributed to atmospheric pollution and the materials used in roofs construction (Huston et al. 2012). In urban areas, public transport is a major source of lead emissions, contributing to its presence in rainwater (Sandroni and Migon 2002). PAHs, which are chemical compounds characterized by ring structures composed of carbon atoms, are another significant pollutant. Some PAHs are potentially carcinogenic and can enter rainwater due to air pollution (Chopek et al. 2016, Mojiri et al. 2019).

Due to the growing issue of water pollution caused by organic micropollutants, scientists are searching for new, effective adsorption materials. Geopolymers have emerged as a promising solution, although further modifications are necessary to enhance their adsorption efficiency (Maleki et al. 2019, Refaie et al. 2020,Yu et al. 2020). Geopolymers show great potential for removing various pollutants from water and wastewater, including heavy metals such as zinc, nickel, lead, copper, chromium, cadmium, manganese and cobalt (Kara et al. 2017, Al-Zboon et al. 2011, Cheng et al. 2012, Sitarz-Palczak 2023, Duan et al. 2016). Their effectiveness stems from active sites on their surface, attributed to the presence of metal oxide groups, which enhance their adsorption capacity for heavy metal ions (Oualit et al. 2022).

Recent studies have explored the production of geopolymers from materials such as fly ash and metakaolin. For example, Duan et al. (2016) developed a porous geopolymer based on fly ash and iron ore to remove Cu(II) from wastewater, achieving an adsorption capacity of 113.41 mg/g at 40 °C and a pH of 6.0. Similarly, Kara et al. (2018) removed heavy metal ions Mn(II) and Co(II) from aqueous solutions, with maximum single-layer adsorption capacities of 72.34 mg/g and 69.23 mg/g, respectively. In another study, Yu et al. (2020) investigated a geopolymer made from metakaolin, reporting maximum adsorption capacity of 108.2 mg/g for Cu(II) and 95.3 mg/g for Cr(VI) in binary systems. These findings underscore the potential of geopolymers as adsorbents and highlight the necessity of continued research to optimize their performance.

Recent research has focused on the incorporation of carbon nanomaterials into geopolymers (Sekkal et al. 2022). Carbon nanotubes, with their unique properties, can significantly increase the adsorption capacity of many adsorbents (Li et al. 2021). Although studies describe the synthesis of nanotube-doped geopolymers, their applications have primarily focused on areas unrelated to pollutant adsorption. Most applications of geopolymers doped with carbon nanotubes are centered on improving concrete performance. To our knowledge, only the work of Yan et al. (2022) has investigated the use of geopolymers for the adsorption of heavy metals and dyes. However, that study was limited to the adsorption of adsorbates from model solutions, which do not accurately simulate the complexities of environmental samples. The novelty of this work lies in the application of the synthesized geopolymer doped with carbon nanotubes for the removal of lead and anthracene from actual rainwater.

Therefore, the aim of this study is to develop a metakaolin-based geopolymer incorporating multi-walled carbon nanotubes functionalized with carboxylic group (GEO+MWCNT) to effectively adsorb both heavy metals and organic micropollutants.

Materials and methods

Materials

All chemical materials used in this study were of analytical grade. Kaolin was obtained from the Aluminum Sulphate Company of Egypt, (Al-Qalyubia Governorate, Egypt). Carboxyl group-functionalized MWCNTs were obtained from Chengdu Organic Chemistry Co. Ltd. (Chengdu, China). Deionized water was supplied by the Ultrapure Lab Water System (Rephile Bioscience Shanghai, China). Acetonitrile (ACN) and methanol (MeOH) were purchased from Avantor Performance Materials (Gliwice, Poland), while anthracene (ANT), H_2SO_4, and NaOH were purchased from Sigma Aldrich (Poznań, Poland). Lead ions concentrations were monitored spectrophotometrically using Merck test kits, and the lead standard solution ($PbCl_2$) was purchased from Merck (Poland).

Preparation of samples

To produce metakaolin, kaolin was calcined at 800 ° C for 3 hours. The preparation of GEO+MWCNT followed these steps: (1) sonication: MWCNT were sonicated in a 1% Brij surfactant solution for 5 minutes, (2) mixing: metakaolin was mixed with a 10 M NaOH solution (solid-to-liquid ratio of 1.3) using a mechanical mixer for 15 minutes (3) MWCNT addition: MWCNTs were added to alkalized metakaolin at a mass ratio of 1:99 (MWCNT: metakaolin), (4) molding and hardening: the slurry of metakaolin and MWCNT was placed in high-temperature-resistant silicone molds and heated in a laboratory dryer at 60ºC for 24 hours for hardening, (5) grinding: the hardened material was ground in a mortar, (6) washing and drying: the ground material was washed with distilled water to remove unreacted sodium hydroxide and then dried at 120°C for 2 h in the laboratory dryer, (7) sieving: the dried material was sieved using a pneumatic screen to obtain particles sized 0.2-0.5 mm. A pristine geopolymer (without MWCNT) was also prepared and used as a reference (control sample). The samples were labelled as follows: GEO for pristine geopolymer and GEO+MWCNT for geopolymer containing MWCNT.

Tab. 1. Physicochemical characteristics of rainwater.

Parameter	Unit	Rainwater (average value)
pH	-	6.28
Conductivity	µS/cm	28.20
Color	mgPt/L	12
Turbidity	FTU	6
COD	mg/L	63
Absorbance UV_{254}	1/cm	0.09
TOC	mg/L	5.10
N-NO_3	mg/L	1.1
P-PO_4	mg/L	1.4

Characteristics of rainwater

Rainwater was collected from the roof of a single-family home during the rainy season in May in Poland. The basic physicochemical properties of raw rainwater are presented in Table 1.

Characterization of adsorbents

The hybrid geopolymer was characterized using the following techniques:

- Surface morphology: the surface morphology of the studied materials was examined using scanning electron microscopy (SEM) with a JSM 6360LA scanning electron microscope manufactured by JEOL (Japan).
- Structural properties: the structural properties, including surface area and pore size distribution, were analyzed using the low-temperature nitrogen adsorption and desorption technique, according to the Brunauer-Emmett-Teller (BET) method.
- Functional groups: functional groups were identified through vibrational spectra analysis using IR spectroscopy. Measurements were conducted using the ATR technique on the FTIR TENSORII spectrometer by Bruker. Operating parameters included an ATR attachment with a diamond crystal, a measurement range of 400-4,000 cm^{-1}, a resolution of 1 cm^{-2}, and 64 repetitions per sample. Two spectra were recorded for each sample.
- Structure and physical properties: X-ray diffraction patterns were analyzed to determine the structure and physical properties of the geopolymer. Measurements were conducted in Bragg-Brentano (Gonio) geometry with qualitative phase analysis. The measurement parameters were as follows: configuration - reflection, wavelength, ferry. X: Kα (Å): 1.54059, Beam Geometry - Parallel:
  Incident Beam: Slit 1/2 °, Soller 0.04 rad., parallel mirror,
  Reflected Beam: Soller 0.04 rad.
- Zeta potential: the zeta potential was determined using the SurPAss electrokinetic analyzer by Anton Paar (Austria). The measurements were conducted using KCL (0.01 M) as the primary electrolyte and changes in pH during titration were made by adding solutions of HCl or NaOH (0.1 M).

Adsorption experiments

Static adsorption experiments were carried out in 100 ml bottles on a shaker set to 300 rpm. Various experimental parameters, such as: contact time (5-480 min), adsorbent dose (0.1-10 g/L), and solution pH (3-10) were tested to assess their influence on Pb (II) removal by geopolymer (GEO) and geopolymer with multi-walled carbon nanotubes (GEO + MWCNT). For all experiments, the solution volume was fixed at 100 ml, with a Pb (II) concentration of 5 mg/L, and the solution pH was maintained 6.4 unless otherwise specified. Specific conditions for individual experiments were as follows: contact time study: the geopolymer dose was set to 4 g/L, adsorbent dose study: the contact time was fixed at 240 minutes, pH influence study: the solution pH was adjusted using 0.1 M HNO_3/NaOH solutions. The next step of the research focused on determining the degree of reduction in the concentration of lead and anthracene ions. The tests were carried out at a constant room temperature using real rainwater solution modified with anthracene (2 mg/L) and lead (5 mg/L). Adsorption tests were carried out with an adsorbent dose of 4 g/L, varying the adsorption time between 5 and 120 minutes. In order to analyze adsorption kinetics of geopolymers, experimental data were evaluated using pseudo-first-order and pseudo-second-order kinetic models, as described by Kamińska and Bohdziewicz (2016). Adsorption isotherms were fitted to three widely used models: the Langmuir model, the Freundlich model, and the Dubinin-Radushkevich model. All calculations applied in this study were previously detailed by Marszałek et al. (2022).

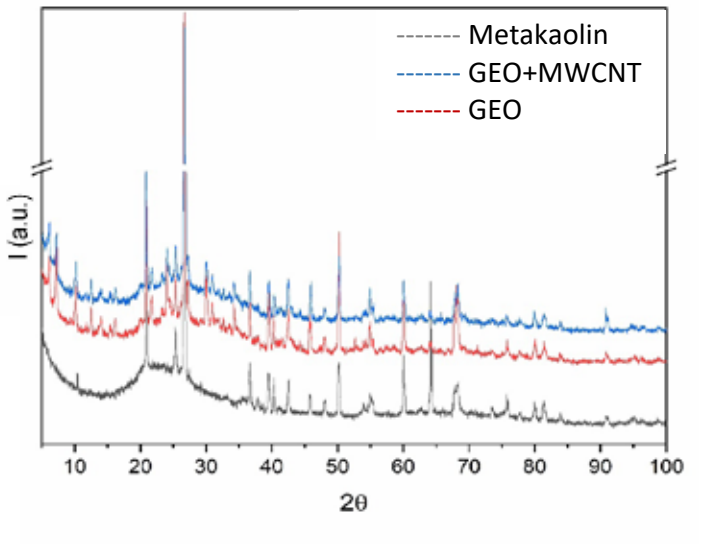

Fig. 1. X-ray diffraction pattern

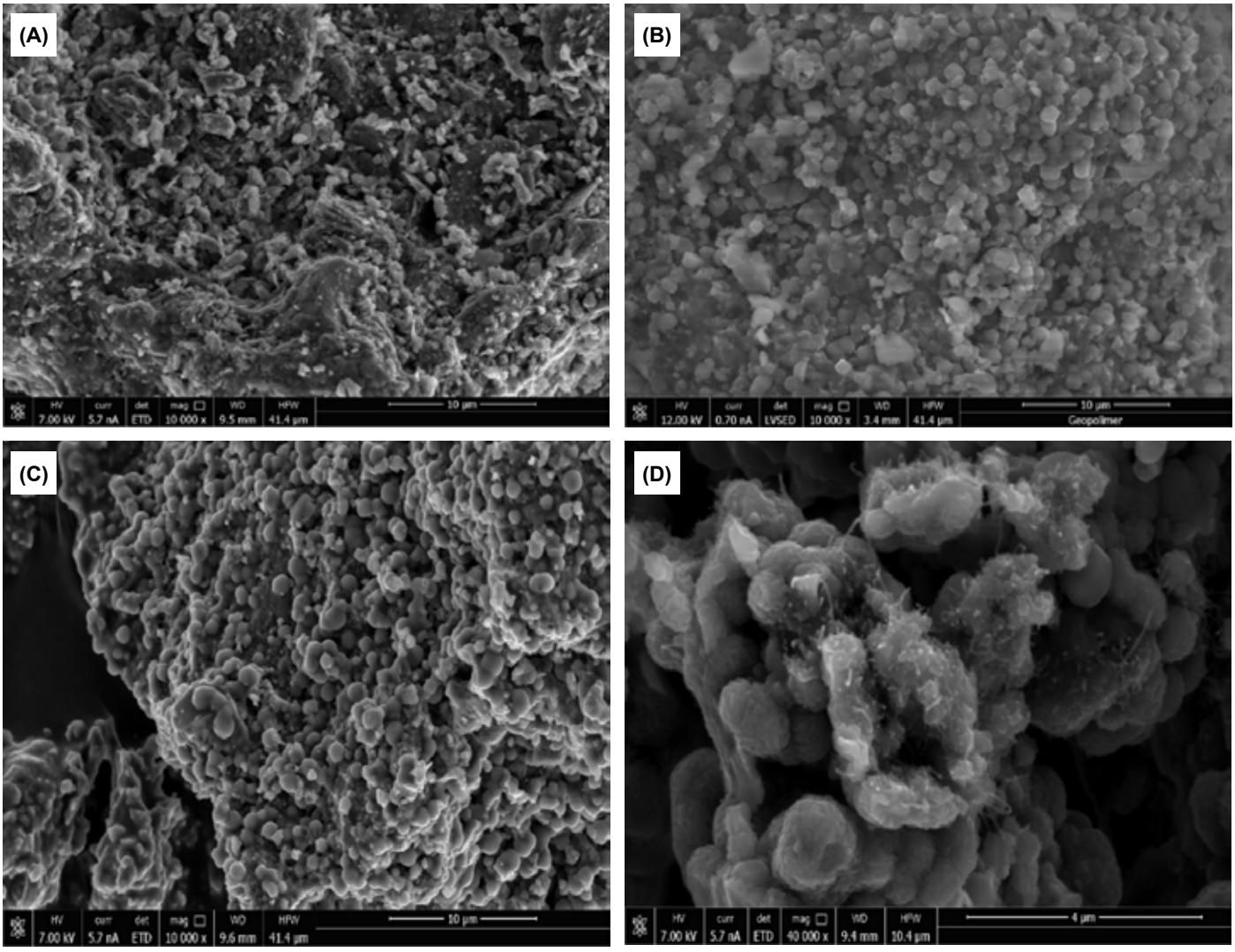

Fig. 2. SEM images of metakaolin (A), geopolymer (B), geopolymer+MWCNT (C, D)

Results and discussion

Discussion of the results of geopolymers characterization

X-ray diffraction (XRD) analysis confirmed the synthesis of the geopolymer. The shift in the broad peak (hump) from 23° to 27° (2θ) between the metakaolin and the geopolymer indicates the progression of the geopolymerization reaction, which is consistent with the literature (Costa et al. 2021, Yang et al. 2022, Niu et al. 2022). This shift reflects structural changes associated with the formation of a new amorphous matrix in the geopolymer. In addition, the structure and physical properties of the geopolymer were evaluated using diffraction data obtained in Bragg-Brentano (Gonio) geometry with qualitative phase analysis. The XRD pattern, presented in Fig. 1 of the manuscript, highlights the characteristic peak shift indicative of geopolymerization, as well as the presence of amorphous phases in the synthesized material.

The surface morphology of the samples is presented in Fig. 2. The surface of metakaolin appears irregular and loose. After the polymerization process, the geopolymer exhibits a morphology characterized by numerous fine particles, which result from the dissolution of metakaolin into the microparticles under the influence of the activating agent. In comparison to metakaolin, both GEO and GEO+MWCNT display a regular and compact surface morphology. The presence of nanotubes is visible in Fig. 2D, where they appear as single threads protruding from the tangled network of nanotubes.

As shown in Fig. 2, the pore size distribution of the samples varied significantly. Metakaolin exhibited the most heterogeneous structure, with a mix of micropores, mesopores, and macropores, which corresponded well with the heterogeneity observed in the SEM images.

In contrast, both GEO and GEO+MWCNT lacked macropores. These samples were predominantly composed of micropores, with a smaller contribution from mesopores. Notably, the incremental surface area attributed to micropores was significantly higher in GEO+MWCNT compared to GEO. The increased microporosity in GEO+MWCNT resulted in the highest specific surface area and total pore area compared to metakaolin and GEO. The addition of MWCNT to GEO+MWCNT led to a substantial increase in surface area, rising from 2.3 to 23.8 m²/g (Table 2 and Fig. 3).

The nitrogen adsorption-desorption isotherms of metakaolin, geopolymer, and geopolymer + MWCNT presented typical features of type II isotherms (Degefu et al. 2022). All adsorbents exhibited H3 hysteresis loops, indicative of mesoporosity in the composite materials (Degefu et al. 2022). The H3 type is characteristic for a groove pores generated from the spaces between platy flake structures. The extent of hysteresis increased with the addition of MWCNT, which can be attributed to the rise in in microporosity (Yan et al. 2022).

Tab. 2. Characteristics of adsorbents from nitrogen sorption-desorption measurements.

Adsorbent	Specific Surface Area (SSA), (m²/g)	Total volume in pores, (mL/g)	Total area in pores, (m²/g)
Metakaolin	8.715	0.03	0.02
Geopolymer	2.28	0.0046	1.523
Geopolymer +MWCNT	23.79	0.015	10.6

The FTIR spectra of metakaolin, GEO and GEO+MWCNT are presented in Fig. 4. (A, B, C). In the FTIR spectrum of metakaolin, a distinct peak at 1066 cm^{-1} corresponds to the asymmetric vibrations of Si-O-Si bonds. A slightly less intense peak at 778 cm^{-1} is attributed to Si-O-Al vibrations, while the peak at 434 cm-1 is associated with Si-O vibrations (Gao et al. 2020). These results confirm the presence of characteristic functional groups without additional bands indicating impurities. For the pure geopolymer, the most intense peak at 980 cm^{-1} corresponds to Si-O stretching vibration. This peak is broad, likely encompassing other Si-O-related vibrations, such as 1100 or 1139 cm^{-1}. A broad band with a maximum at 3384 cm^{-1} and a small peak at 1651 cm^{-1} are attributed to O-H vibrations from adsorbed water molecules. According to the literature, vibration bands assigned to Secondary Building Units (SBU) are observed in the range of 800–550 cm^{-1}. SBUs consist of linked tetrahedral SiO_4 and AlO_4 units forming various rings (Kljajevica et al. 2017). In the FTIR spectrum measured for the geopolymer with the addition of multi-walled carbon nanotubes (MWCNT), the peak positions are nearly identical to those of the pure geopolymer. However, a notable difference is the change in the intensity of the peak at 1651 cm^{-1}, resulting from O-H vibrations of particles adsorbed on the surface. This variation suggests that MWCNT is attached to the geopolymer at these sites.

The zeta potential is crucial in assessing the surface charge and the effect on the adsorption mechanisms. Fig. 4D presents the zeta potential curves of the geopolymers and the influence of pH on lead adsorption. Across the studied pH range (2-10), the GEO + MWCNT geopolymer exhibited a much lower zeta potential compared to GEO. For example, at pH around 7, the zeta potential was positive (4.2 mV) for GEO, whereas GEO+MWCNT showed a negative zeta potential (-14 mV). Consequently, the isoelectric point (IP) was shifted from 7.15 (GEO) to 2.9 (GEO+MWCNT). The higher negative zeta potential and lower IP for GEO+MWCNT are attributed to the presence of carboxylic groups on the surface of carbon nanotubes, which become dissociated under alkaline conditions. It is also clear that such a significant change in the zeta potential can affect adsorption mechanism and the removal efficiency of Pb (II) (Wan et al. 2021).

Effect of adsorbent dose and time on adsorption of lead

The effect of GEO and GEO+MWCNT doses on lead adsorption in rainwater was investigated (Fig. 5 A). The results indicate that the increased availability of sorption sites on the surface of GEO+MWCNT is crucial for effective adsorption. At lower doses, GEO+MWCNT showed higher efficacy in removing lead from rainwater compared to GEOs, attributed to the increased active surface area and unique properties of carbon nanotubes, which enhance the sorption capacity of geopolymers (Abbas et al., 2016). As the sorbent dose increases, more active sites become available, initially improving the

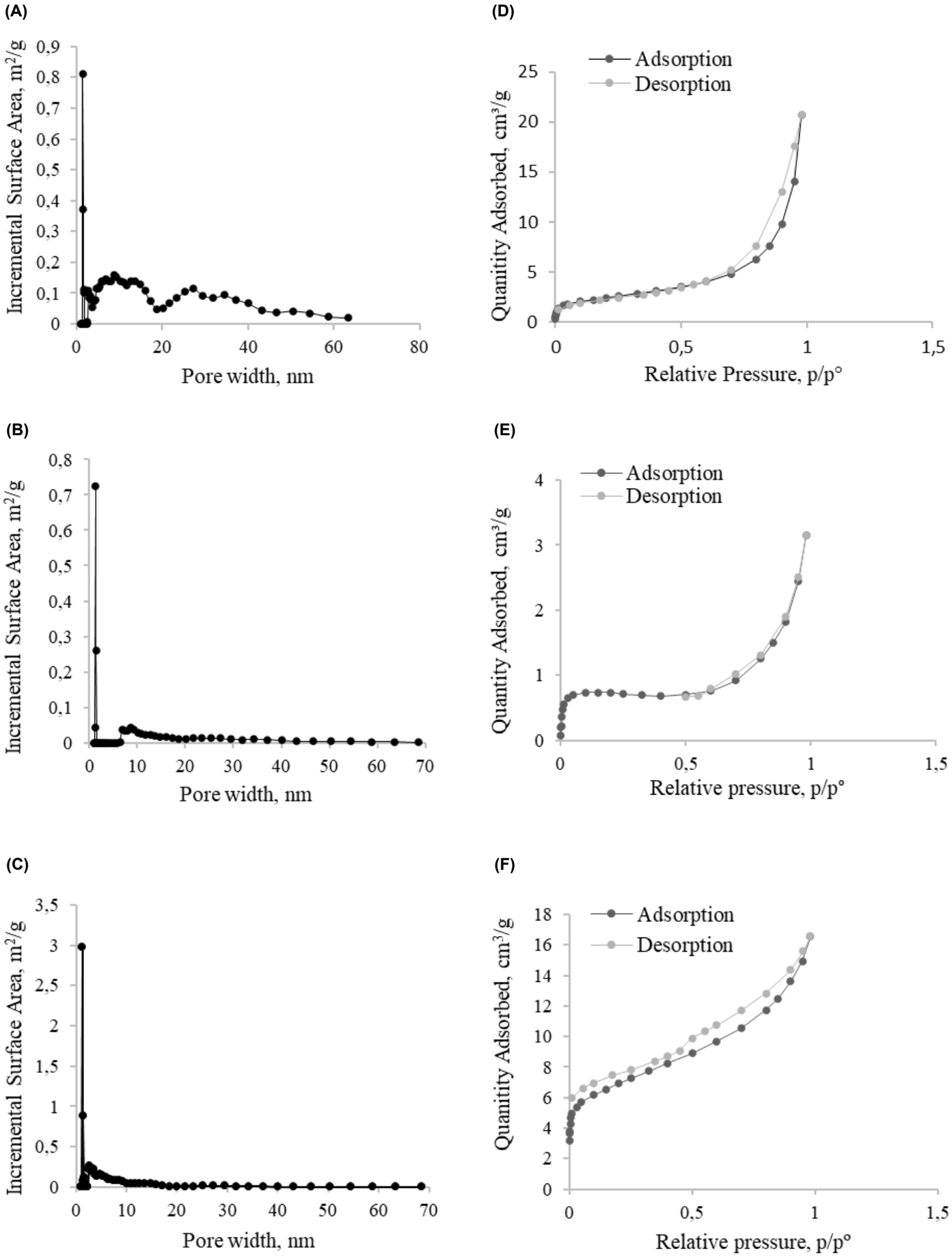

Fig. 3. Pore size distribution of metakaolin (A), geopolymer (B), geopolymer+MWCNT (C) and sorption-desorption isotherms of metakaolin (C), geopolymer (D), geopolymer+MWCNT (E)

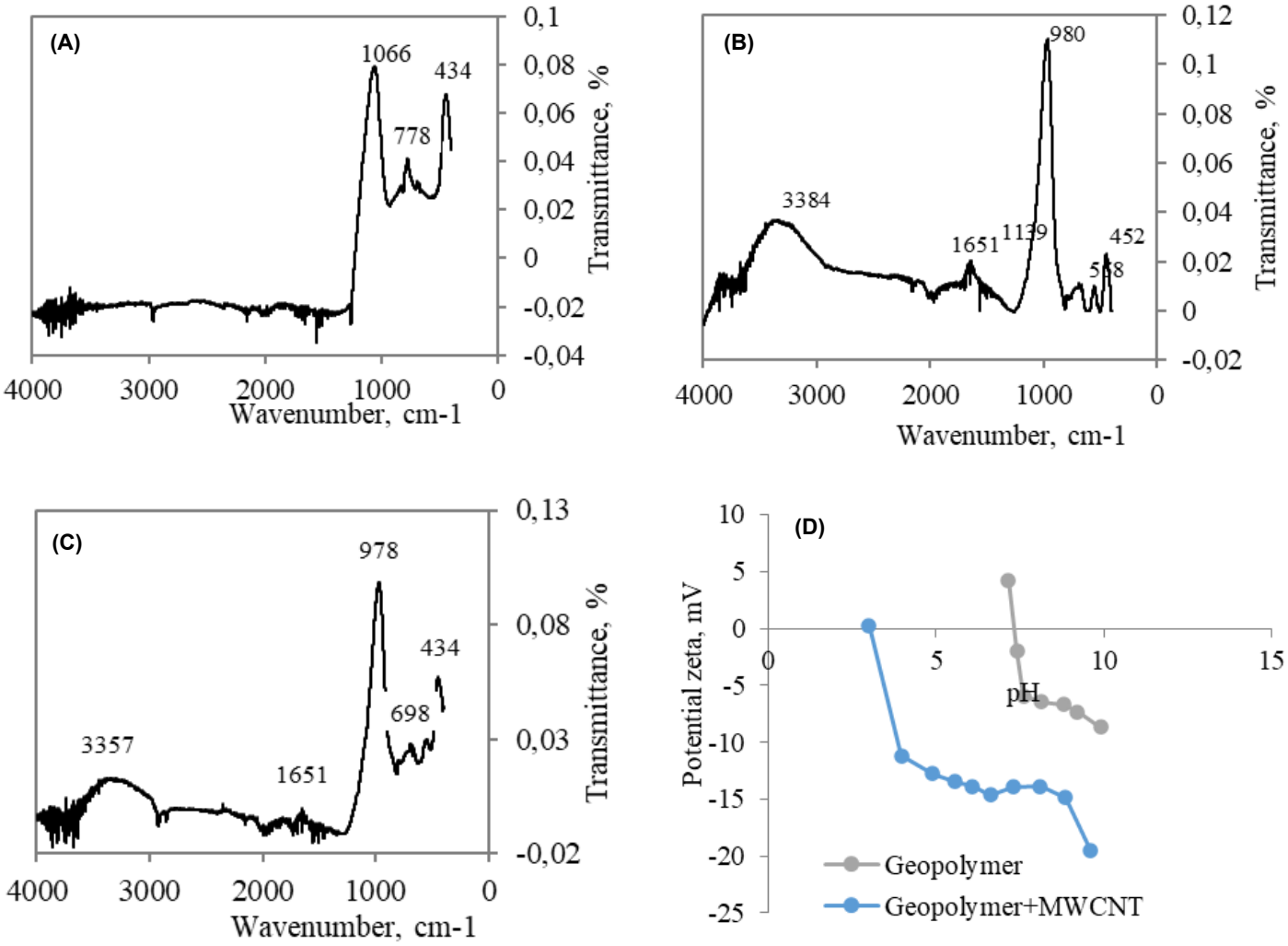

Fig. 4. FTIR spectrum of metakaolin (A), geopolymer (B), geopolymer with MWCNT (C) and zeta potential curves of geopolymers (D)

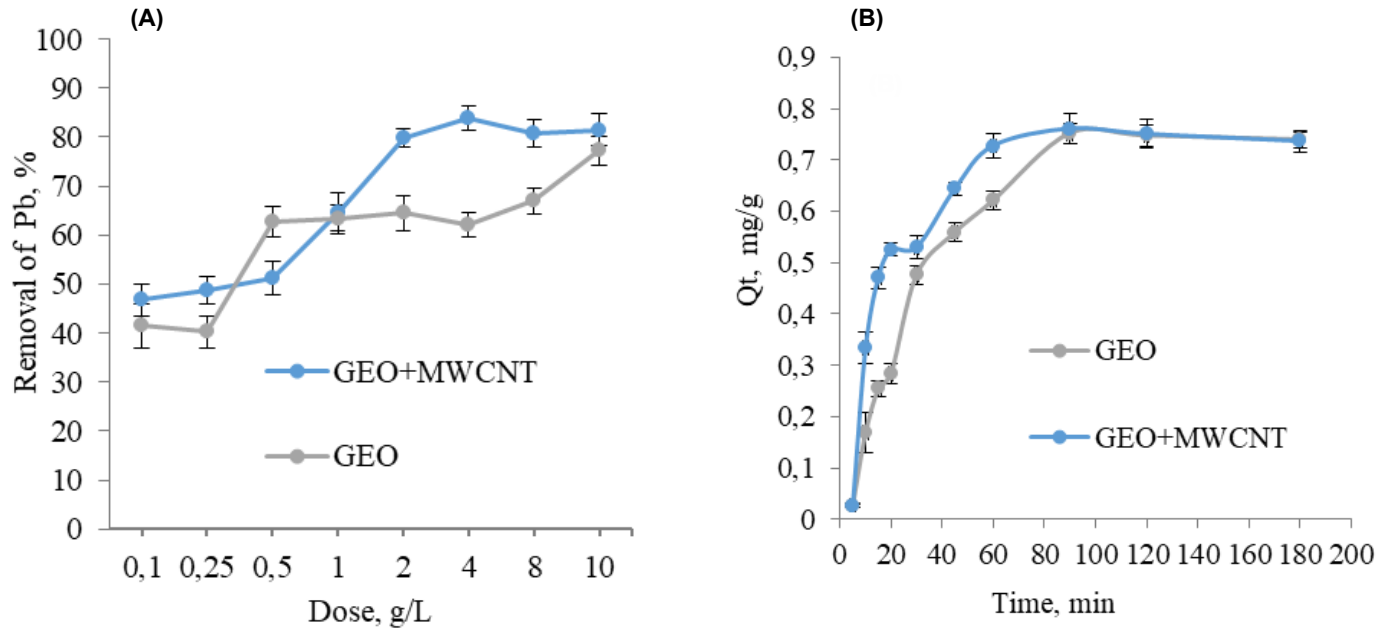

Fig. 5. Effect of type and dose of adsorbent on lead removal (A), adsorbed amount of lead as a function of time for GEO and GEO+MWCNT (B), C_0 = 4 mg/L

efficiency of adsorption. However, at the highest doses, no significant differences were observed between the effectiveness of the geopolymer with and without nanotubes. This suggests that the sorption surface reaches its maximum capacity beyond a certain dose, and further increases in sorbent do not lead to an increase in adsorption efficiency due to saturation of active sites and the limited amount of impurities in the solution (Li et al., 2013, Sitarz-Palczak, 2023). Once the saturation occurs, further increasing the amount of sorbent does not result in efficiency improvements, as the available impurities are unable to fully utilize the additional adsorption sites.

Contact time was found to be a significant factor influencing the effectiveness of heavy metal ion adsorption by the adsorbent. Results from the batch experiment (Fig. 5B) show that lead adsorption was initially very rapid and then gradually slowed down. The literature also indicates a rapid initial adsorption rate, which is associated with the high availability of active sites that become saturated over time (Foo and Hameed, 2010). As adsorption sites fill, the process slows, reaching equilibrium after 90 minutes. Similar results were observed in studies on other heavy metal adsorbent materials, where the equilibrium time ranged from 60 to 120 minutes (Gautam et al., 2014).

Influence of rainwater pH on adsorption

The adsorption capacity of lead on the surface of adsorbents is influenced by the pH of the aqueous solution (Fig. 6.).

It was found that at low pH, metal uptake decreases due to an increase in positive charge density (protons) on the adsorbent surface. For the geopolymer, the maximum adsorption was achieved at a pH range of 6.0-7.0, beyond which the adsorption efficiency declined. In contrast, GEO + MWCNT showed increased lead removal with rising pH, reaching maximum efficiency at pH 8. The reduced uptake of heavy metals at low pH can be attributed to competition for adsorption sites between the higher concentrations of H+ ions (from the solution) and heavy metal ions. At low pH, protonation of the adsorbent's functional groups creates a positively charged surface, causing electrostatic repulsion of metal ions. At higher pH, lower H+ concentration and reduced surface protonation result in a more negative surface charge, which enhances adsorption through electrostatic attraction between the positively charged metals and negatively charged surface.

The adsorption of heavy metals is closely related to the surface charge of the adsorbent. Zeta potential measurements showed that the zero point of charge (ZPC) for GEO and GEO+MWCNT was 7.15 and 2.9, respectively. At pH 7 (pH > pH ZPC), the surface deprotonates, creating a negative charge that increases electrostatic attraction between the surface of the adsorbent and Pb(II). The actual pH of rainwater was selected for further studies, as adsorption at this pH is high while preventing the precipitation of metal ions such as hydroxides or metal oxides, which form at solution pH > 6 (Wan et al., 2021, Al-Zboon et al., 2017).

Furthermore, at low pH (<4), the high concentration of H+ promotes protonation of the geopolymer surface, resulting in the repulsion of Pb (II). This trend is consistent for both adsorbents (Moungam et al., 2022). In addition to surface sorption, cation exchange between monovalent alkaline cations (Na+) and metal cations Pb(II) may also occur (Moungam et al., 2022). However, the primary sorption mechanism involves chemical interactions between metal ions and the surface functional groups of geopolymers. Protons in the carboxyl groups of MWCNTs are exchanged with metal ions in the aqueous phase. During Pb(II) adsorption, these interactions between the functional groups of the geopolymers and Pb(II) lead to enhanced adsorption properties. The addition of MWCNT to the geopolymer significantly increases Pb(II) adsorption compared to the geopolymer alone, due to the larger specific surface area provided by MWCNT (Zhang et al., 2022, Qu et al., 2022).

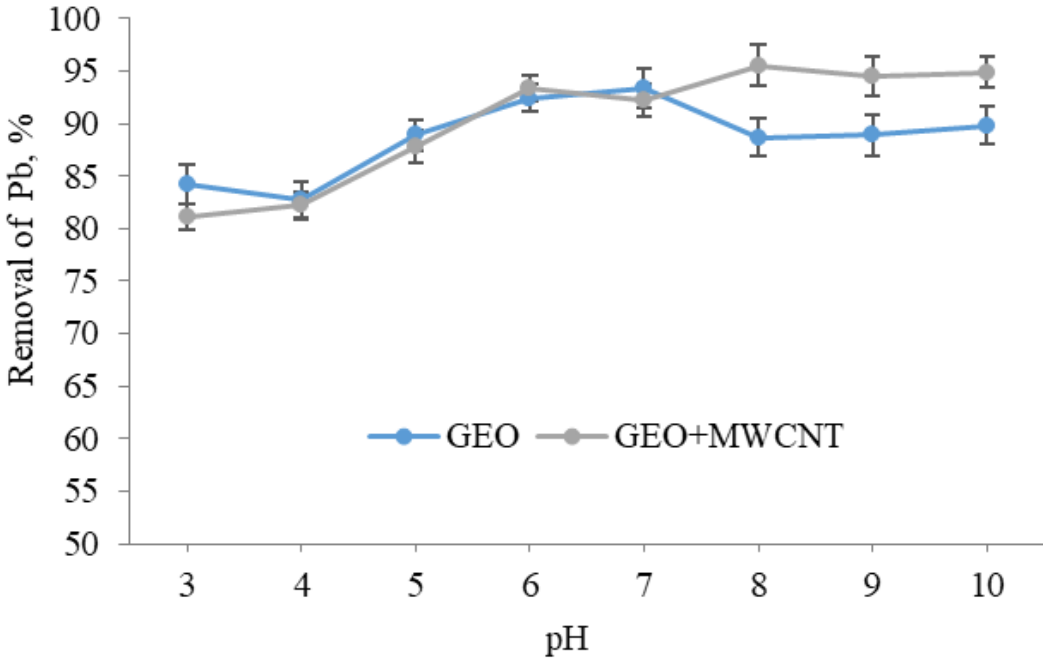

Fig. 6. Impact of rainwater pH on lead adsorption

Effectiveness of lead and anthracene adsorption of pollutants from rainwater

The next stage of the research focused on evaluating the simultaneous removal efficiency of lead and anthracene. Experiments were carried out at constant room temperature using real rainwater modified with 2 mg /L of anthracene and 5 mg/L of lead. Adsorption tests were performed with a fixed dose of 4 g/L and varying adsorption times ranging from 5-120 minutes. The results are shown in Fig. 7.

For the geopolymer, anthracene adsorption remained constant at an average of 70%, regardless of the process duration. In contrast, the geopolymer with MWCNT showed increasing anthracene removal over time, reaching 100% within 60 minutes of the process. Such a high degree of removal is caused by the addition of MWCNT, which is characterised by a large specific surface area comparable to the specific surface of activated carbon. Therefore, the oxidation process further improves dispersibility and introduces oxygen-containing functional groups such as -COOH, -OH, and -C double bond of O on the CNT surface. These functional groups increase the negative charge on the carbon surface and provide lone pairs of electrons to interact with metal ions, thereby enhancing cation exchange capacity (Rao et al. 2007).

These results confirm that modifying the geopolymer with MWCNT is a promising strategy to improve its adsorption capacity, especially for removing anthracene from rainwater. The study assessed the simultaneous removal of lead and anthracene and compared their adsorption from single-adsobate solutions. It was found that both pollutants compete for adsorption sites, with lead ions exerting a greater impact on reducing adsorption effectiveness compared to anthracene. Similar observations were made by Zhang et al. (2018), who

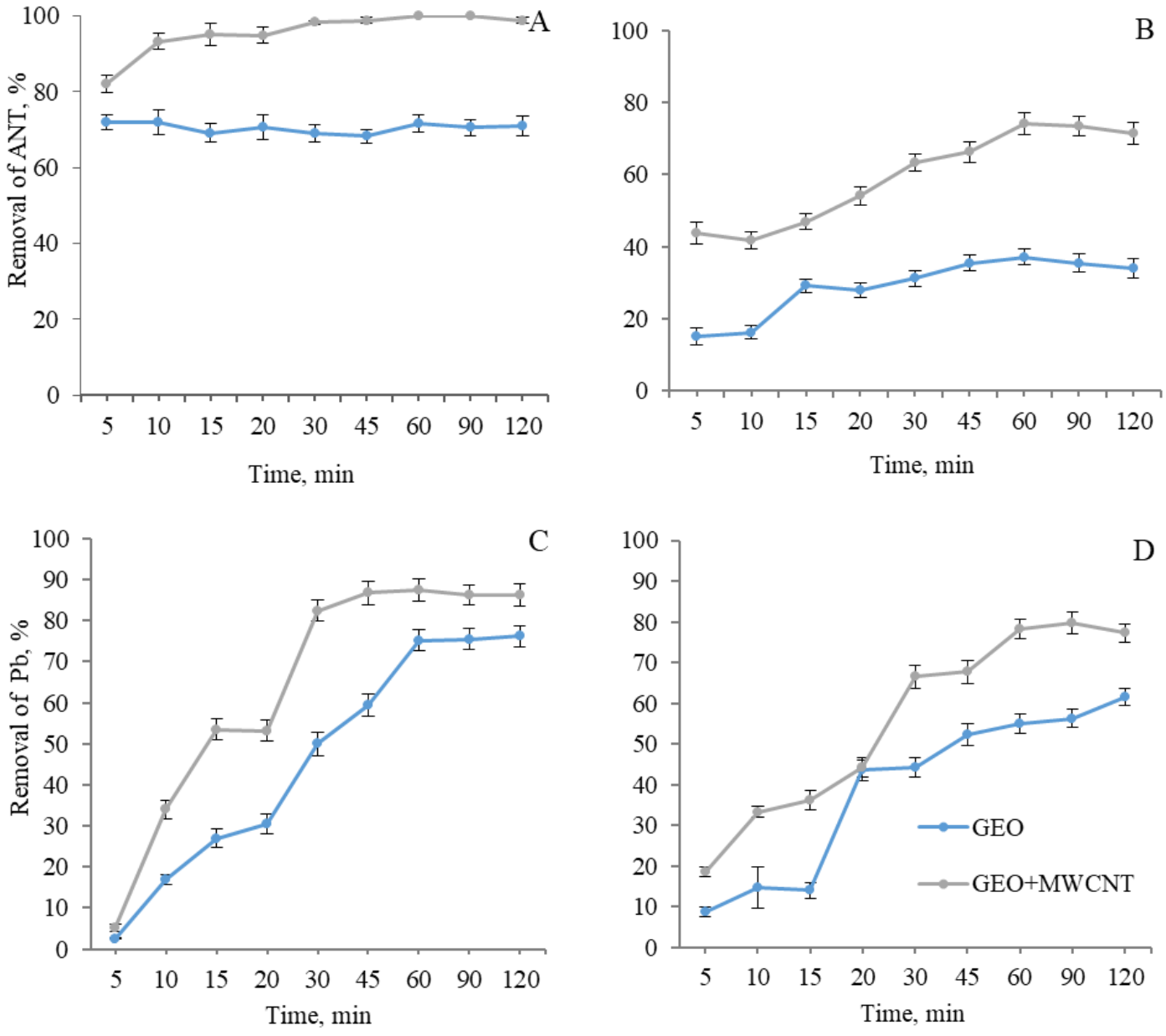

Fig. 7. Removal of anthracene and lead removal by GEO and GEO + MWCNT from soultion containing one and two adsorbates: Anthracene removal in the absence of Pb (II) (A) in the presence of Pb (II) (B), Lead removal in the absence of anthracene (C) and in the presence of anthracene (D) depending on the time

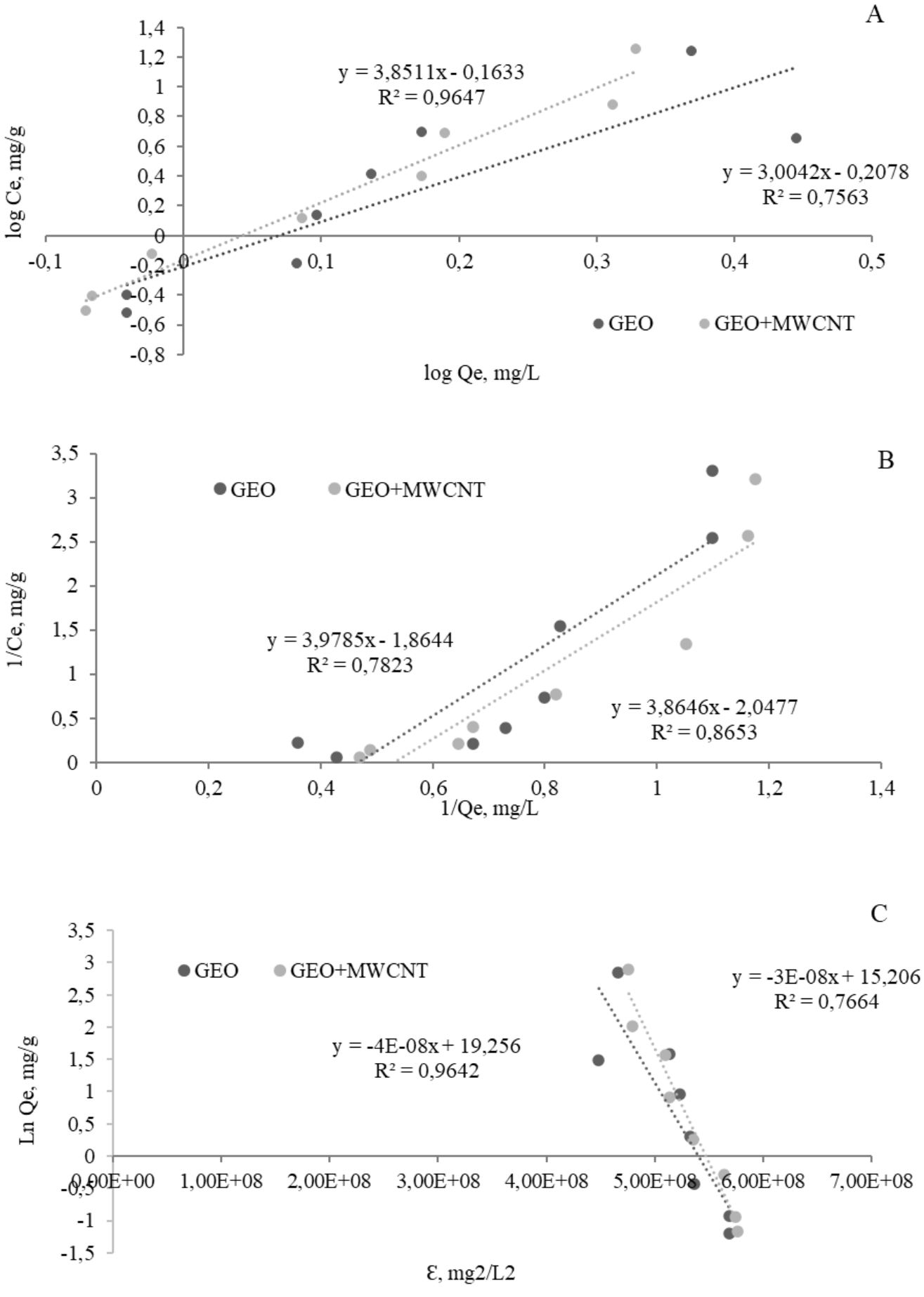

Fig. 8. Freundlich (A), Langmuir (B), and Dubinin-Radushkevich (C) isotherms of Pb (II) on GEO and GEO+MWCNT

investigated a composite with reduced graphene oxide derived from biochar from corn straw. Their study on the competitive adsorption of lead and atrazine revealed that lead reduced atrazine adsorption, while atrazine had no effect on lead adsorption (Zhang et al. 2018).

In solutions containing both metal ions and organic compounds, a decrease in lead adsorption efficiency was observed. After 60 minutes, GEO+MWCNT removed 78.2% of lead in the anthracene-containing solution, compared to 86.7% in rainwater without anthracene. Anthracene had a smaller impact on Pb(II) removal than Pb(II) ions had on anthracene adsorption. While GEO+MWCNT achieved 100% anthracene removal from rainwater without lead, the efficiency dropped to 74% in the presence of Pb(II) ions.

Studies have shown that the adsorption capacity of both adsorbates in a binary solution is lower compared to single-component systems. This was confirmed in research by Cheng et al. on Cu(II) and cyromazine (Cheng et al. 2021). However, by the 90th minute of the process, the adsorption efficiency levelled out. The process using GEO showed a 20% reduction in lead adsorption efficiency in the presence of anthracene over the entire time interval. Additionally, anthracene removal by GEO decreased by 50% - 80% (5-120 min) in the binary solution compared to the sinlge-anthracene solution. These results suggest that anthracene has a smaller effect on lead removal than lead ions have on anthracene adsorption.

Adsorption isotherms

Adsorption isotherms are crucial for understanding the interaction between the adsorbate and adsorbent at equilibrium. Analyzing these data facilitates matching them to the appropriate model, thereby optimizing the adsorption process (Adewoye et al. 2021). For Pb(II) adsorption on GEO and GEO+MWCNT, three isothermal models were evaluated: Langmuir, Freundlich and Dubinin-Radushkevich (Fig. 8, Table 3).

A comparison of correlation coefficients (R^2) showed that for GEO, the data fit poorly with the models analyzed, indicating a greater complexity in the adsorption processes. The R^2 values for the Langmuir, Freundlich, and Dubinin-Radushkevich models were 0.76, 0.78, and 0.77, respectively, suggesting that Pb(II) adsorption on GEO is not ideally described by these isotherms. On the other hand, the results for GEO+MWCNT were more conclusive. The Freundlich and Dubinin-Radushkevich models showed higher correlation coefficients (0.96 and 0.965), indicating more complex, multilayer adsorption on a heterogeneous surface. This aligns with the role of carbon nanotubes in increasing the number of active sites. The R^2 value for Langmuir was 0.86, which also suggests the presence of some features of monolayer adsorption. The Dubinin-Radushkevich model's adsorption energy values (E) were less than 8 kJ/mol for both GEO and GEO+MWCNT, indicating that Pb(II) adsorption process is physical and driven by van der Waals and electrostatic interactions. For GEO+MWCNT, the energy value of 5 kJ/mol further confirmed the physical nature of this process (Mobasherpour et al. 2014).

The mechanism of lead adsorption can be explained by both physisorption and chemisorption, suggesting that adsorption occurs according to the monolayer chemisorption model on heterogeneous surfaces (Wan et al. 2021). Similar complexity is observed in studies of other metals, such as Cu(II) and Cr(VI), absorbed on a metakaolin geopolymer, where the Langmuir and Freundlich models both provide good fits (Yu et al. 2020). In the literature, heavy metal adsorption on geopolymers is often described using Freundlich isotherms, suggesting multilayer adsorption on heterogeneous surfaces. On the other hand, adsorption involving ion exchange reactions is often described by the Langmuir model, highlighting monolayer chemisorption as the dominant mechanism (Wan et al. 2021). In our study, experimental data for Pb(II) adsorption on GEO and GEO+MWCNT align better with the Freundlich and Dubinin-Radushkevich models, indicating heterogeneous adsorption. The Freundlich n-factor of less than 1 indicates a relatively low interaction intensity between Pb(II) and the adsorbents. In summary, the Freundlich and Dubinin-Radushkevich models best describe Pb(II) adsorption on GEO+MWCNT, suggesting a more complex mechanism involving a heterogeneous surface. The Langmuir model, on the other hand, better explains the saturation point of the adsorbent surface, where further increases in sorbent dose do not enhance adsorption efficiency.

Kinetics of adsorption

Adsorpion of lead on GEO and GEO + MWCNT followed the second-order kinetic model as R2 values were close to unity. Furthermore, the calculated values of Qt (cal) are similar to the values of the experimental data Qt (exp) (Table 4).

This model is often more effective in describing the adsorption of heavy metals, such as lead, on materials with a large specific surface area. For lead adsorption (Pb(II)), our results showed that the pseudo-second-order model provides a better fit to the adsorption kinetics, suggesting the dominance of chemisorption. This suggests that ionic interactions between Pb(II) ions and active adsorption sites on the geopolymer play a significant role (Manyangadze et al. 2020). Similarly, for anthracene adsorption, kinetic analysis confirms that the

Tab. 3. Parameters of Freundlich, Langmuir, and Dubinin-Radushkevich equations, and the correlation coefficients for the adsorption of Pb (II) on the studied adsorbents.

Adsorbent	Langmuir			Freundlich			Dubinin-Radushkevich		
	Q_m (mg/g)	K_L (L/mg)	R^2 (-)	K_F ((mg/g) L/mg)^n)	n (-)	R^2 (-)	E (J/mol)	aDR (mg/g)	R^2 (-)
GEO	4.602	0.698	0.780	1.613	0.332	0.76	5773.5	4016815	0.76
GEO+ MWCNT	6.798	0.560	0.860	1.456	0.259	0.965	5000	2305549	0.96

Tab. 4. Parameters for the pseudo-first and second order kinetic model for the adsorption of Pb (II) and anthracene on GEO and GEO+MWCNT.

	Pseudo-First- Order Equation Parameters			Pseudo-Second-Order Equation Parameters		
			Pb (II)			
Adsorbate	**K_1 (1/min)**	**Qe (mg/g)**	**R^2**	**K_2 (g/(mg•min))**	**Qe (mg/g)**	**R^2**
GEO	0.0005	19.25	0.296	0.21	0.58	0.988
GEO+MWCNT	0.0005	16.47	0.235	0.33	0.85	0.920
			Anthracene			
GEO	0.0002	16.83	0.49	0.95	0.15	0.997
GEO+MWCNT	0.0004	15.45	0.905	0.7	0.31	0.998

pseudo-second-order model better describes the adsorption process, further supporting the role of chemisorption-type interactions. The effectiveness of anthracene adsorption may be attributed to π-π interactions and van der Waals forces between the carbon nanotubes (MWCNTs) and the aromatic rings of anthracene (Yu et al. 2020).

Conclusions

The aim of this study was to evaluate the effectiveness of removing organic contaminants, such as anthracene and heavy metals from a multicomponent solution. Research on mixed adsorption systems involving real multicomponent solutions remain relatively limited. The main conclusions of this study are following:

1. X-ray diffraction (XRD) measurements were performed to confirm the successful synthesis of the geopolymer. The shift of the hump from 23° to 27° (2θ) indicated the occurence of the geopolymerization reaction, confirming the proper preparation of the adsorbent. Incorporating MWCNTs into the geopolymer increased the specific surface area (BET), reaching 23.79 m^2/g. It was 10 times larger than that of the pure geopolymer.
2. For the geopolymer, the best results were obtained for a pH in the range of 6.0 to 7.0, beyond which the efficiency declined. On the other hand, the geopolymer with MWCNT-COOH addition showed an increase in lead removal efficiency with an increase in pH was found. The best effectiveness was obtained at pH 8.
3. At lower doses of adsorbents, the addition of carbon nanotubes to the geopolymer resulted in higher adsorption efficiency. However, at the highest doses tested, no significant difference was found in the effectiveness of lead removal from rainwater.
4. The Freundlich and Dubinin-Radushkevich models best describe Pb(II) adsorption on GEO+MWCNT, suggesting a more complex adsorption mechanism involving a heterogeneous surface. On the other hand, the Langmuir model better explained the saturation point of the adsorbent surface, where further increase in the dose of the sorbent did not lead to an increase in adsorption efficiency.
5. The adsorption process reached equilibrium within 90 minutes. Then, the lead adsorption rate decreased as a result of the reduction in sorption sites. The calculated values corresponded well with the experimental data. This suggests that both the lead and anthracen adsorption followed second-order kinetics on GEO and GEO + MWCNT.
6. The degree of anthracene removal from the solution without lead was 100%, while in rainwater containing Pb (II) ions, the adsorption efficiency decreased by 26%. This suggests that the presence of heavy metals in water reduces the adsorption of micropollutants. Conversely, micropollutants present in water can affect the adsorption of lead.
7. The modification of the geopolymer with carbon nanotubes (MWCNTs) significantly improved the adsorption efficiency of both lead and anthracene, due to improved surface properties and a greater availability of adsorption sites.

Acknowledgments

This research was supported by the Excellence Initiative - Research University program at the Silesian University of Technology (2021) and funded by the Polish Ministry of Science and Higher Education (2024).

References

Abbas, A., Al-Amer, A.M., Laoui, T., Al-Marri, M.J., Nasser, M. S., Khraisheh, M. & Atieh, M.A. (2016). Heavy metal removal from aqueous solution by advanced carbon nanotubes: critical review of adsorption applications. *Separation and Purification Technology,* 157, pp. 141-161. DOI: 10.1016/j.seppur.2015.11.039

Adewoye, T.L, Ogunleye, O.O, Abdulkareem, A.S, Salawudeen, T.O. & Tijani, J.O (2021) Optimization of the adsorption of total organic carbon from produced water using functionalized multi-walled carbon nanotubes. *Heliyon*, 7(1), e05866. DOI:10.1016/j.heliyon.2020.e05866.

Albidah, A., Alghannam, M., Abbas, H., Almusallam, T. & Al-Salloum Y (2021) Characteristics of metakaolin-based geopolymer concrete for different mix design parameters. *Journal of Materials Research and Technology*, 10, pp. 84-98. DOI:10.1016/j.jmrt.2020.11.104.

Al-Zboon, K., Al-Harahsheh, M.S. & Hani, F.B. (2011) Fly ash-based geopolymer for Pb removal from aqueous solution. *Journal of Hazardous Materials*, 188(1-3), pp. 414-421. DOI:10.1016/j.jhazmat.2011.01.133.

Al-Zboon, K.K., Al-Smadi, B.M. & Al-Khawaldh, S. (2017) Erratum to: Natural Volcanic Tuff-Based Geopolymer for Zn Removal: Adsorption Isotherm, Kinetic, and Thermodynamic Study. *Water Air Soil Pollut* 228, 164. DOI:10.1007/s11270-017-3335-3.

Cheng, H., Liu, Y. & Li, X. (2021) Adsorption performance and mechanism of iron-loaded biochar to methyl orange in the presence of Cr6+ from dye wastewater. *Journal of Hazardous Materials,* 415, 125749. DOI: 10.1016/j.jhazmat.2021.125749.

Cheng, M.C. & You, C.F. (2010) Sources of major ions and heavy metals in rainwater associated with typhoon events in southwestern Taiwan. *Journal of Geochemical Exploration*, 105(3), pp. 106-116. DOI:10.1016/j.gexplo.2010.04.010.

Cheng, T.W., Lee, M.L., Ko, M.S., Ueng, T.H. & Yang, S.F. (2012) The heavy metal adsorption characteristics on metakaolin-based geopolymer. *Applied Clay Science*, 56, pp. 90-96. DOI:10.1016/j.clay.2011.11.027.

Cheng, Z., Liu, Z., Hao, H., Lu, Y. & Li, S. (2022) Multi-scale effects of tensile properties of lightweight engineered geopolymer composites reinforced with MWCNTs and steel-PVA hybrid fibers. *Construction and Building Materials*, 342, 128090. DOI:10.1016/j.conbuildmat.2022.128090.

Chłopek, Z., Suchocka, K., Dudek, M. & Jakubowski, A. (2016) Hazards posed by polycyclic aromatic hydrocarbons contained in the dusts emitted from motor vehicle braking systems. *Archives of Environmental Protection*, 42 (3), pp. 3-10. DOI:10.1515/aep-2016-0033.

Costa, L.M., Almeida, N.G.S., Houmard, M., Cetlin, P.R., Silva, G.J.B. & Aguilar, M.T.P. (2021) Influence of the addition of amorphous and crystalline silica on the structural properties of metakaolin-based geopolymers. *Applied Clay Science*, 215, 106312. DOI:10.1016/j.clay.2021.106312.

Degefu, D.M., Liao, Z., Berardi, U. & Labbé, G. (2022) The effect of activator ratio on the thermal and hygric properties of aerated geopolymers. *Journal of Building Engineering*, 45, 103414. DOI:10.1016/j.jobe.2021.103414.

Duan, P., Yan, C., Zhou, W. & Ren, D. (2016) Development of fly ash and iron ore tailing based porous geopolymer for removal of Cu (II) from wastewater. *Ceramics International*, 42 (12), pp. 13507-13518. DOI:10.1016/j.ceramint.2016.05.143.

Eldos, H.I., Zouari, N., Saeed, S. & Al-Ghouti, M.A. (2022) Recent advances in the treatment of PAHs in the environment: Application of nanomaterial-based technologies. *Arabian Journal of Chemistry*, 15 (7), 103918. DOI:10.1016/j.arabjc.2022.103918.

Foo, K.Y. & Hameed, B.H. (2010) Insights into the modeling of adsorption isotherm systems. *Chemical Engineering Journal*, 156 (1), pp. 2-10. DOI:10.1016/j.cej.2009.09.013.

Gao, L., Zheng, Y., Tang, Y., Yu, J., Yu, X. & Liu, B. (2020) Effect of phosphoric acid content on the microstructure and compressive strength of phosphoric acid-based metakaolin geopolymers, *Heliyon* 6, e03853. DOI:10.1016/j.heliyon.2020.e03853.

Huston, R., Chan, Y.C., Chapman, H., Gardner, T. & Shaw, G. (2012) Source apportionment of heavy metals and ionic contaminants in rainwater tanks in a subtropical urban area in Australia. *Water Research*, 46 (4), pp. 1121-1132. DOI:10.1016/j.watres.2011.12.008.

Jin, H., Zhang, Y., Wang, Q., Chang, Q. & Li, C. (2021) Rapid removal of methylene blue and nickel ions and adsorption/desorption mechanism based on geopolymer adsorbent. *Colloid and Interface Science Communications*, 45, 100551. DOI:10.1016/j.colcom.2021.100551.

Kamińska, G. & Bohdziewicz, J. (2016) Potential of various materials for adsorption of micropollutants from wastewater *Environment Protection. Engineering*, 42, pp. 161-178. DOI:10.5277/epe160413.27.

Kara, I., Tunc, D., Sayin, F. & Akar, S.T. (2018) Study on the performance of metakaolin based geopolymer for Mn (II) and Co (II) removal. *Applied Clay Science*, 161, pp. 184-193. DOI:10.1016/j.clay.2018.04.027.

Kara, İ., Yilmazer, D. & Akar, S.T. (2017) Metakaolin based geopolymer as an effective adsorbent for adsorption of zinc (II) and nickel (II) ions from aqueous solutions. *Applied Clay Science*, 139, pp. 54-63. DOI:10.1016/j.clay.2017.01.008.

Khanal, G., Thapa, A., Devkota, N. & Paudel, U.R. (2020) A review on harvesting and harnessing rainwater: an alternative strategy to cope with drinking water scarcity. *Water Supply*, 20 (8), pp. 2951-2963. DOI:10.2166/ws.2020.264.

Li, Y., Du, Q., Liu, T., Peng, X., Wang, J., Sun, J., Wang, Y., Wu, S., Wang, Z., Xia, Y. & Xia, L. (2013). Comparative study of methylene blue dye adsorption onto activated carbon, graphene oxide, and carbon nanotubes. *Chemical Engineering Research and Design*, 91(2), pp. 361-368. DOI:10.1016/j.cherd.2012.07.007

Li, F., Yang, Z., Chen, D., Lu, Y., & Li, S. (2021). Research on mechanical properties and micro-mechanism of Engineering Geopolymers Composites (EGCs) incorporated with modified MWCNTs. *Construction and Building Materials,* 303, 124516. DOI:10.1016/j.conbuildmat.2021.124516.

Li, Y., Cheng, X., Liu, K., Yu, Y. & Zhou, Y. (2022). A new method for identifying potential hazardous areas of heavy metal pollution in sediments. *Water Research,* 224, 119065. DOI:10.1016/j.watres.2022.119065.

Li, P. (2020). Mechanical properties and micro characteristics of fly ash-based geopolymer paste incorporated with waste Granulated Blast Furnace Slag (GBFS) and functionalized Multi-Walled Carbon Nanotubes (MWCNTs). *Journal of Hazardous Materials*, 401, 123339. DOI: 10.1016/j.jhazmat.2020.123339.

Makar, J., Margeson, J. & Luh, J. (2005). Carbon nanotube/cement composites-early results and potential applications. In *Proceedings of the 3rd international conference on construction materials: performance, innovations and structural implications.* pp. 1–10). Vancouver, Canada.

Maleki, A., Hajizadeh, Z., Sharifi, V. & Emdadi, Z. (2019). A green, porous and eco-friendly magnetic geopolymer adsorbent for heavy metals removal from aqueous solutions. *Journal of Cleaner Production,* 215, pp. 1233–1245. DOI:10.1016/j.jclepro.2019.01.084.

Manyangadze, M., Chikuruwo, N.M., Narsaiah, T.B., Chakra, C.S., Charis, G., Danha, G. & Mamvura, T.A. (2020). Adsorption of lead ions from wastewater using nano silica spheres synthesized on calcium carbonate templates. *Heliyon,* 6(11), e05309. DOI:10.1016/j.heliyon.2020.e05309.

Marszałek, A., Kamińska, G. & Salam, N.F.A. (2022). Simultaneous adsorption of organic and inorganic micropollutants from rainwater by bentonite and bentonite carbon nanotubes composites. *Journal of Water Process Engineering,* 46, 102550. DOI:10.1016/j.jwpe.2021.102550.

Mobasherpour, I., Salahi, E. & Ebrahimi, M. (2014). Thermodynamics and kinetics of adsorption of Cu(II) from aqueous solutions onto multi-walled carbon nanotubes. *Journal of Saudi Chemical Society,* 18(6), pp. 792–801. DOI:10.1016/j.jscs.2011.09.006.

Mojiri, A., Zhou, J.L., Ohashi, A., Ozaki, N. & Kindaichi, T. (2019). Comprehensive review of polycyclic aromatic

hydrocarbons in water sources, their effects and treatments. *Science of the Total Environment,* 696, 133971. DOI:10.1016/j.scitotenv.2019.133971.

Moungam, L.M.B., Tchieda, K.V., Mohamed, H., Pecheu, N.C., Kaze, R.C., Kamseu, E. & Tonle, I.K. (2022). Efficiency of volcanic ash-based porous geopolymers for the removal of Pb^{2+}, Cd^{2+}, and Hg^{2+} from aqueous solution. *Cleaner Materials*, 5, 100106. DOI:10.1016/j.clema.2022.100106.

Murat-Błażejewska, S. & Błażejewski, R. (2020). Converting sewage holding tanks to rainwater harvesting tanks in Poland. *Archives of Environmental Protection*, 46(4), pp. 121–131. DOI:10.24425/aep.2020.135770

Niu, X., Elakneswaran, Y., Islam, C.R., Provis, J.L. & Sato, T. (2022). Adsorption behaviour of simulant radionuclide cations and anions in metakaolin-based geopolymer. *Journal of Hazardous Materials*, 429, 128373. DOI:10.1016/j.jhazmat.2022.128373.

Oualit, M. & Irekti, A. (2022). Mechanical performance of metakaolin-based geopolymer mortar blended with multi-walled carbon nanotubes. *Ceramics International*, 48(11), pp. 16188–16195. DOI:10.1016/j.ceramint.2022.02.166.

Qu, G., Zhou, J., Liang, S., Li, Y., Ning, P., Pan, K. & Tang, H. (2022). Thiol-functionalized multi-walled carbon nanotubes for effective removal of Pb^{2+} from aqueous solutions. *Materials Chemistry and Physics*, 278, 125688. DOI:10.1016/j.matchemphys.2021.125688.

Rao, G.P., Lu, C. & Su, F. (2007). Sorption of divalent metal ions from aqueous solution by carbon nanotubes: A review. *Separation and Purification Technology*, 58 (1), pp. 224–231. DOI:10.1016/j.seppur.2006.12.006.

Refaie, F.A.Z., Abbas, R. & Fouad, F.H. (2020). Sustainable construction system with Egyptian metakaolin-based geopolymer concrete sandwich panels. *Case Studies in Construction Materials*, 13, e00436. DOI:10.1016/j.cscm.2020.e00436.

Sandroni, V. & Migon, C. (2002). Atmospheric deposition of metallic pollutants over the Ligurian Sea: Labile and residual inputs. *Chemosphere*, 47(7), pp. 753–764. DOI:10.1016/S0045-6535(01)00337-X.

Sekkal, W. & Zaoui, A. (2022). High strength metakaolin-based geopolymer reinforced by pristine and covalent functionalized carbon nanotubes. *Construction and Building Materials*, 327, 126910. DOI:10.1016/j.conbuildmat.2022.126910.

Sijal, A.A., Shamsuddin, M.R., Rabat, N.E., Zulfiqar, M., Man, Z. & Low, A. (2019). Fly ash-based geopolymer for the adsorption of anionic surfactant from aqueous solution. *Journal of Cleaner Production*, 229, pp. 232–243. DOI:10.1016/j.jclepro.2019.04.384.

Sitarz-Palczak, E. (2023). Study of Zn(II) ion removal from galvanic sludge by geopolymers. *Archives of Environmental Protection,* 49(4), pp. 11–20. DOI:10.24425/aep.2023.148681.

Tan, W., Li, Y., Ding, L., Wang, Y., Li, J., Deng, Q., Guo, F. & Xiao, X. (2019). Characteristics and metal leachability of natural contaminated soil under acid rain scenarios. *Archives of Environmental Protection*, 45(2), pp. 91–98. DOI: 10.24425/aep.2019.126698.

Wan, J., Zhang, F., Han, Z., Song, L., Zhang, C. & Zhang, J. (2021). Adsorption of Cd^{2+} and Pb^{2+} by biofuel ash-based geopolymer synthesized by one-step hydrothermal method. *Arabian Journal of Chemistry*, 14(8), 103234. DOI:10.1016/j.arabjc.2021.103234.

Yan, S., Ren, X., Zhang, F., Huang, K., Feng, X. & Xing, P. (2022). Comparative study of Pb^{2+}, Ni^{2+}, and methylene blue adsorption on spherical waste solid-based geopolymer adsorbents enhanced with carbon nanotubes. *Separation and Purification Technology*, 284, 120234. DOI:10.1016/j.seppur.2021.120234.

Yang, J., Xu, L., Wu, H., Jin, J. & Liu, L. (2022). Microstructure and mechanical properties of metakaolin-based geopolymer composites contain high volume of spodumene tailings. *Applied Clay Science*, 218, 106412. DOI:10.1016/j.clay.2022.106412.

Yu, Z., Song, W., Li, J. & Li, Q. (2020). Improved simultaneous adsorption of Cu(II) and Cr(VI) of organic modified metakaolin-based geopolymer. *Arabian Journal of Chemistry*, 13(3), pp. 4811–4823. DOI:10.1016/j.arabjc.2020.01.001.

Zhang, X., Yuan, N., Xu, S., Li, Y. & Wang, Q. (2022). Efficient adsorptive elimination of organic pollutants from aqueous solutions on ZIF-8/MWCNTs-COOH nanoadsorbents: Adsorption kinetics, isotherms, and thermodynamic study. *Journal of Industrial and Engineering Chemistry,* 111, pp.155-167. DOI:10.1016/j.jiec.2022.03.048.-

Zhang, Y., Cao, B., Zhao, L., Sun, L., Gao, Y., Li, J. & Yang, F. (2018). Biochar-supported reduced graphene oxide composite for adsorption and coadsorption of atrazine and lead ions. *Applied Surface Science*, 427, pp. 147–155. DOI:10.1016/j.apsusc.2017.07.237.

Udoskonalanie geopolimerów wielościennymi nanorurkami węglowymi do jednoczesnej adsorpcji ołowiu i antracenu z wody deszczowej.

Streszczenie. Celem badań było przygotowanie i ocena skuteczności geopolimeru domieszkowanego wielościennymi nanorurkami węglowymi funkcjonalizowanymi grupami karboksylowymi (GEO+MWCNT) w usuwaniu ołowiu i antracenu (ANT) z wód opadowych. Przeprowadzone procesy adsorpcyjne pozwoliły określić skuteczność usuwania jonów ołowiu i antracenu, dobrać dawkę adsorbentu i czas procesu, a także określić wpływ pH roztworu na skuteczność adsorpcji. W badaniach skupiono się także na charakterystyce geopolimerów (potencjał SEM, BET, FTIR, XRD, XRF, ZETA), izotermach adsorpcji i kinetyce adsorpcji. Charakterystyka GEO+MWCNT wykazała zwiększoną powierzchnię właściwą i mikroporowatość w porównaniu z nieskazitelnym geopolimerem (GEO). Eksperymenty adsorpcyjne wykazały, że GEO+MWCNT osiągnął wyższą skuteczność usuwania Pb(II) i ANT w porównaniu z GEO. Maksymalne usunięcie ołowiu i antracenu przez GEO+MWCNT wyniosło odpowiednio 100% i 87,5%, natomiast dla GEO 71,5% i 76,2%. W przypadku GEO+MWCNT usunięcie ołowiu osiągnęło 78,2% w roztworach zawierających antracen i 86,7% w wodach deszczowych wolnych od antracenu. Optymalne usuwanie Pb(II) nastąpiło przy pH 8 dla GEO+MWCNT. Kinetyka adsorpcji była zgodna z modelem pseudodrugiego rzędu, wskazując na złożony mechanizm obejmujący adsorpcję fizyczną, chemisorpcję i przyciąganie elektrostatyczne. Odkrycia te sugerują, że geopolimery, szczególnie w połączeniu z MWCNT-COOH, mają znaczny potencjał zastosowania w procesach oczyszczania wody deszczowej.